In Situ Synthesis of 2-Phenylbenzimidazole as an Hydrogen Sulfide Corrosion Inhibitor of Carbon Steel

Sh. Pournazari,‡, M.H. Moayed,* and M. Rahimizadeh***

ABSTRACT

Hydrogen sulfide corrosion inhibition of carbon steel has been evaluated using the combination of benzene-1,2-diamine, benzaldehyde, and $FeCl_3$ to in situ inhibitor synthesis at 25°C using electrochemical and weight-loss studies. The results showed that the corrosion rate of steel decreased significantly by increasing the inhibitor concentration. The concentration of in situ synthesized inhibitor was measured by ultraviolet and visible spectrophotometer (UV-vis). The morphology and composition of the corrosion products were analyzed using scanning electron microscopy (SEM)/energy-dispersive spectroscopy (EDS). Fourier transform infrared spectroscopy (FTIR) demonstrated the formation of 2-phenylbenzimidazole on the surface by an in situ manner. Quantum chemical studies were applied to investigate the correlation between the molecular structure and inhibition effect of this compound.

KEY WORDS: carbon steel, electrochemical investigations, Fourier transform infrared spectroscopy, hydrogen sulfide corrosion, inhibitor

INTRODUCTION

Corrosion is one of the most serious problems in the oil and gas production and transportation industry. Oilfield corrosion manifests itself in several forms, such as carbon dioxide corrosion (sweet corrosion) and hydrogen sulfide corrosion (sour corrosion).[1-3] As sweet fields are being depleted and higher oil prices make it possible for profitable development of sour oil and gas fields, a tremendous concern in the production and transportation sour oil and gas is the corrosion caused by the acid gases carbon dioxide and hydrogen sulfide.[4] Even though corrosion-resistant alloys (CRA) have long been available as a material selection option that mitigates carbon dioxide and hydrogen sulfide corrosion, carbon steel is in general more cost-effective for oil and gas facilities and, hence, is the most widely used material option.[4-5] So, H_2S corrosion is one of the main factors of the corrosive destruction observed in steel equipment and pipelines that has been investigated for many years.[1,3-7] The internal corrosion of carbon steel pipeline in the presence of carbon dioxide and hydrogen sulfide was recognized first in the 1940s and has been investigated for more than 60 years.[8] During oil-producing operations, an intense growth of sulfate-reducing bacteria (SRB), which generate H_2S, takes place as a result of an injection of surface water into petroleum reservoirs. This leads to microbial and H_2S corrosion of equipment.[9] In the literature, there are studies of the electrochemical behaviors of both steel[10] and iron[11-14] in the solutions with hydrogen sulfide. The results demonstrated that in some cases. Hydrogen sulfide could inhibit the corrosion of iron under certain special conditions such as lower hydrogen sulfide concentration (≤0.04 mmol dm^{-3}) and pH values of 3 to 5, but, in most cases, hydrogen suflide could accelerate both the anodic iron dissolution and the cathodic hydrogen evolution.[3-4,12-13] The injection of a corrosion

Submitted for publication: October 2, 2012. Revised and accepted: June 14, 2013. Preprint available online: July 1, 2013, doi: http://dx.doi.org/10.5006/0854.

‡ Corresponding author. E-mail: sh.pournazari@gmail.com.
* Metallurgical and Material Engineering Department, Faculty of Engineering, Ferdowsi University of Mashhad, Mashhad 91775-1111, Iran.
** Chemistry Department, Faculty of Science, Ferdowsi University of Mashhad, Mashhad 91775-1111, Iran.

ISSN 0010-9312 (print), 1938-159X (online)
13/000213/$5.00+$0.50/0

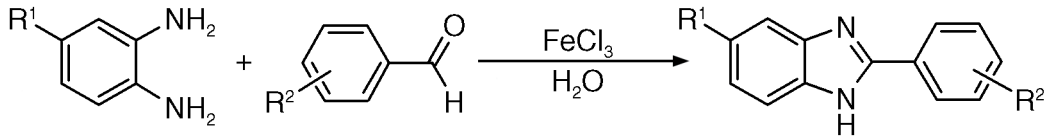

FIGURE 1. *Synthetic route of in situ synthesized inhibitor.*

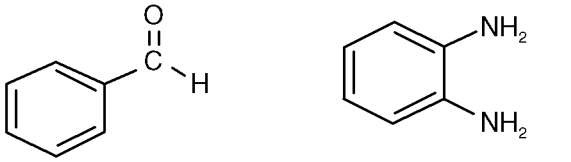

FIGURE 2. *Molecular structure of investigated compounds.*

inhibitor is a standard practice in oil and gas production systems to control internal corrosion of carbon steel structures because it is cost-effective and flexible.[3,6,9,15] A wide variety of organic compounds has been tested as hydrogen sulfide corrosion inhibitors.[9] Among these compounds nitrogen-based organic inhibitors such as imidazolines or their salts have been used successfully in these applications even without an understanding of the inhibition mechanism.[1] So, the widespread interest in benzimidazole-containing structures has prompted extensive studies for their synthesis. On the whole, the procedures that lead to synthesis of this structure have some considerable difficulties.[16] Studies report that the adsorption of the organic inhibitors mainly depends on some factors such as its functional groups and electronic density of donor atoms;[1,3] adsorption is also supposed to depend on the possible interaction of the π orbitals of the inhibitor with the d orbitals of the surface atoms.[17-18]

Following our recent research involving the combination of 2-phenylbenzimidazole components as an in situ synthesized corrosion inhibitor in acidic solution,[19] the purpose of this paper was to evaluate the admixture of benzaldehyde and benzene-1,2-diamine along with ferric chloride catalyst according to Figure 1 as a hydrogen sulfide corrosion inhibitor of carbon steel by using electrochemical and gravimetric measurements. Additionally, ultraviolet and visible spectrophotometer (UV-vis), Fourier transform infrared spectroscopy (FTIR), quantum chemical method, scanning electron microscopy (SEM), and energy-dispersive spectroscopy (EDS) have been used in this work.

EXPERIMENTAL PROCEDURES

Specimen Preparation and Experimental Setup

Material tested was a carbon steel with a chemical composition (in wt%) of: 0.13% C, 0.51% Mn, 1.5% Cr, 0.31% Si, 0.023% P, 0.010% Al, 1.55% Ni, and Fe balance. The working electrode was a rod-like electrode with an exposed area of 7 cm^2. Prior to each experiment, electrodes were mechanically abraded down to 1200 grit abrasive silicon carbide (SiC) paper, then washed with distilled water, cleaned ultrasonically by ethanol, and dried in a compressed warm air flow. Electrochemical measurements have been carried out in a typical three-electrode cell configuration with a saturated calomel electrode (SCE) as a reference electrode, a large piece of platinum wire as an auxiliary electrode, and a carbon steel specimen as a working electrode. A reference electrode with a 4 mm diameter tip sealed into the reaction vessel cap was inserted directly into the test solution. A flow of nitrogen gas above the test solution water line was used throughout the test period. The temperature of electrolyte solutions was controlled with a bath at 25°C (within ±2°C accuracy).

Inhibitor and Electrolyte Solution Preparation

In this study benzene-1,2-diamine and benzaldehyde were purchased from a commercial supplier. 2-phenylbenzimidazole was synthesized from the combination of benzene-1,2-diamine and benzaldehyde using ferric hydrogen sulfate ($Fe[HSO_4]_3$) as catalyst by Eshghi, et al.[20] Since only ferric ions were important for this reaction and ferric hydrogen sulfate was really difficult to produce, in this study ferric chloride was used instead because it is more available and cheaper. It is necessary to mention that the same procedure has already been performed by other researchers.[21] The molecular structures of the investigated compounds are given in Figure 2. To produce the in situ synthesized inhibitor, ferric chloride as catalyst was purchased from a commercial supplier.

To reach the in situ synthesized inhibitor, different concentrations of benzene-1,2-diamine and benzaldehyde with the same concentration of ferric chloride as the reactions catalyst[19] were mixed using 20 cm^{-3} dimethyl sulfoxide (DMSO) at room temperature. However, dimethyl sulfoxide adds solubility only and does not provide additional corrosion protection. Concentrations of the composition used in this work were 10^{-5}, 10^{-4}, and 10^{-3} mol/L. The testing solution consists of 3% sodium chloride (NaCl) solution, deaerated with nitrogen gas (N_2) for 1 h, and H_2S was produced in the sealed system by reacting 3.53 g L^{-1} sodium sulfide (Na_2S) with 1.7 g L^{-1} acetic acid (CH_3COOH) according to the following reaction:

$$Na_2S + 2CH_3COOH \rightarrow 2NaCH_3COO + H_2S \quad (1)$$

which leads to generate 0.5 g L^{-1} H_2S concentration.[3,15] In this case the resulting pH level was 2.6.

Electrochemical Measurements

The electrochemical tests have been performed using a laboratory potentiostat. Before each test, the working electrode was immersed for 1 h in solution to obtain a steady-state open-circuit potential. Linear polarization resistance tests have been accomplished at a constant sweep rate (10 mV/min) with a scanning range from –15 mV to 15 mV around open-circuit potential. The polarization resistance values have been measured by calculating the slope of the linear part of current-potential plot. Electrochemical impedance spectroscopy (EIS) measurements have been carried out in frequency range of 100 kHz to 0.01 Hz with an amplitude of 15 mV peak-to-peak using alternating current signals at open-circuit potential. Potentiodynamic polarization was conducted at a constant sweep rate of 30 mV/min and a scanning range of –350 mV to 350 mV around the open-circuit potential. The value of surface coverage (θ) and the percentage of inhibition efficiency (%η) were calculated using the following equation:

$$\theta = \frac{i^{o}_{corr} - i_{corr}}{i^{o}_{corr}} \quad (2)$$

$$\%\eta = \theta \times 100 \quad (3)$$

where i^{o}_{corr} and i_{corr} are corrosion current densities of carbon steel in the absence and presence of inhibitor, respectively.

Weight-Loss Experiment

Specimens were cut into 2 by 5 by 0.37 cm for immersion tests and three specimens used for each series were measured for good reproducibility. The samples were weighed before exposure using a digital balance with a precision of 0.001 g for the original weight (W_0). After immersion for 2.5 h in the H_2S-contained solution in the absence and presence of in situ synthesized inhibitor, the corroded specimens were taken out from the solutions, cleaned with distilled water, and dried. Finally, the samples were weighed again to obtain the final weight (W_i). The corrosion rate (r) (mg cm^{-2} h^{-1}) was calculated via Equation (4).

$$r = \frac{W_o - W_i}{A \times t} \quad (4)$$

where W_0 and W_i are the original weight and final weight of specimens, respectively; A (cm^2) is the exposed surface area of specimens; t (h) represents the immersion time. The inhibition efficiencies were calculated from Equation (5):

$$(\%)\theta = \frac{r_0 - r_1}{r_0} \times 100 \quad (5)$$

where r_0 and r_1 are the values of corrosion rate of carbon steel in uninhibited and inhibited solutions, respectively.

Ultraviolet and Visible Spectrophotometer

A UV spectrophotometer was used for UV-vis spectral measurements. A series of inhibited solutions were prepared with a fixed concentration of the components (10^{-5}, 10^{-4}, and 10^{-3} M). The absorption spectra of these solutions were determined.

Corrosion Attack Morphology and Corrosion Products Investigation

To investigate the effect of inhibitors on corrosion morphology and to analyze the compositions of corrosion products, SEM and EDS were used.

Fourier Transform Infrared Spectroscopy

To indicate the compound that was created on the metal surface by in situ synthesis of the inhibitor, a deposited layer on the metal surface was investigated using FTIR spectra in a FTIR spectrophotometer.

Quantum Chemical Study

The molecular structure of 2-phenylbenzimidazole, benzaldehyde, and benzene-1,2-diamine have been geometrically optimized by the DFT method using B3LYP level and 3-21G** basis set with Gaussian 98[†]. Quantum chemical parameters such as the highest occupied molecular orbital (HOMO) and the lowest unoccupied molecular orbital (LUMO) have been calculated.

RESULTS AND DISCUSSION

Potentiodynamic Polarization Curves of Carbon Steel in H_2S-Containing Solutions and Thermodynamic Calculations

The UV-vis adsorption spectrum of the 10^{-3} M concentration of the component's solution is shown in Figure 3. Similar figures were also obtained for 10^{-4} M and 10^{-5} M but are not summarized here. As it can be seen, the concentration of the in situ synthesized inhibitor were determined by UV-vis measurement at the spectra maximum adsorption wavelength of the product (λ_{max} = 295 nm) according to Figure 3.

Figure 4 shows the potentiodynamic polarization curves of carbon steel in hydrogen sulfide-containing solutions at 25°C in the absence and presence of various concentrations of in situ synthesized inhibitor. It can be understood that the cathodic and anodic branches of polarization curves in hydrogen sulfide-containing solution and hydrogen sulfide-containing solutions with 10^{-5} M inhibitor were very similar, indi-

[†] Trade name.

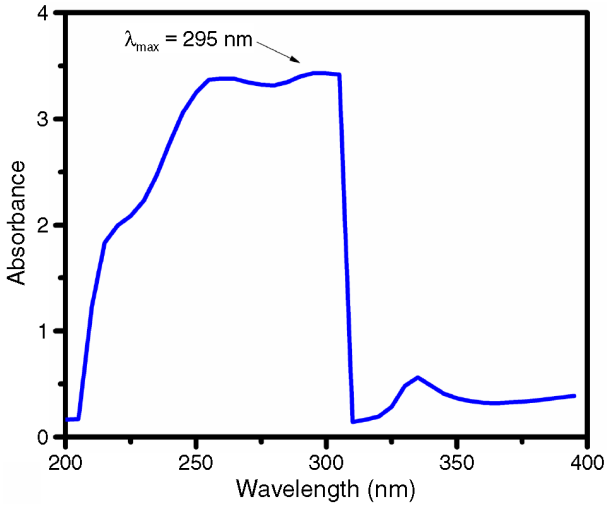

FIGURE 3. *UV-vis spectrum of the 10^{-3} M concentration of the components' solution.*

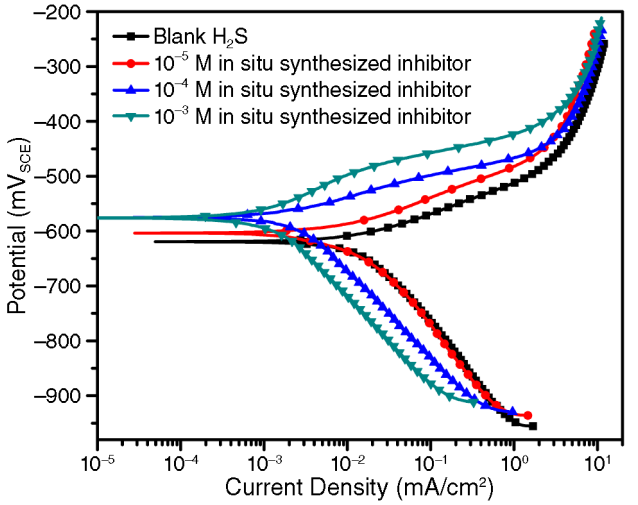

FIGURE 4. *Polarization curves for carbon steel in H_2S-containing solutions at various concentrations of in situ synthesized inhibitor at 25°C.*

cating that the inhibitor could not perform corrosion protection at low concentrations.

There is a parallel shift toward lower currents in both the anodic and cathodic portions of the polarization curves for all concentrations of the inhibitor. This behavior shows that the mechanism of reduction reactions remains unchanged in the case of adsorption on the electrode surface, and the inhibition of the corrosion reaction occurs only because of the blocking of the electrode surface.[9] Adsorption of organic inhibitor molecules onto a metal surface and therefore retarding of metal dissolution and as a consequence hydrogen evolution by blocking available sites is widely accepted by other researchers.[18-19,22-23]

For the anodic part of polarization curves for 10^{-4} M and 10^{-3} M concentrations, initially, the corrosion current densities increased with the potential shifting positively, which means that the adsorption rate is higher than the desorption rate and the adsorption process controls the anodic reaction. When the polarization potential moved positively to about –500 mV, desorption of the inhibitor occurred and corrosion current densities increased markedly as compared with the initial stage. As the potential passed approximately –450 mV, the polarization behavior resembled that in blank solution, which implies that inhibitor thoroughly desorbed from the surface.[19,24]

Electrochemical parameters include corrosion potential (E_{corr}), cathodic and anodic Tafel slopes (β_c and β_a), and corrosion current density (i_{corr}) obtained from the polarization curves in the solution with H_2S were measured by Tafel extrapolation of the anodic and cathodic lines and shown with their standard deviation in Table 1. As it is seen, the low amount of standard deviations indicates that the measurements are repeatable and the differences are not significant. The values of surface coverage (θ) and the percentage of inhibition efficiency (%η) were calculated using Equations (2) and (3).

By increasing inhibitor concentration, the corrosion potential clearly became more positive (from –618 mV_{SCE} in the blank solution to –576 mV_{SCE} in the H_2S-containing solution with the 0.001 M in situ synthesized inhibitor). The value of a corrosion potential is influenced by two processes: the cathodic and

TABLE 1

Electrochemical Parameters Obtained from the Polarization Curves of Different Concentrations of In Situ Synthesized Inhibitor and Weight-Loss Results

		Polarization						Weight Loss	
Inhibitor	Concentration	E_{corr} (mV_{SCE})	i_{corr} (mA/m^2)	β_a (mV/decade)	$-\beta_c$ (mV/decade)	θ	%η	Corrosion Rate (mg cm^{-2} h^{-1})	%Inhibition Efficiency After 2.5 h
Blank		–618 (±18)	0.135 (±1×10^{-2})	52	185	—	—	0.635 (±6×10^{-3})	—
In situ synthesized inhibitor	10^{-5} M	–603 (±8)	0.076 (±8×10^{-3})	52	183	0.44	44	—	—
In situ synthesized inhibitor	10^{-4} M	–576 (±8)	0.012 (±8×10^{-3})	46	157	0.91	91	—	—
In situ synthesized inhibitor	10^{-3} M	–576 (±3)	0.005 (±5×10^{-4})	65	159	0.96	96	0.079 (±9×10^{-3})	87

anodic processes.[25-26] In general, there are two causes of a positive shift of the corrosion potential; either the cathodic process on the metal surface is promoted or the anodic process is restrained.[25] While the cathodic branches were more similar in all concentrations than anodic ones, anodic dissolution of iron is more dominant. Hence, in situ synthesized inhibitor acts as a mixed-type inhibitor with predominant control of anodic reaction.[24]

In addition to electrochemical parameters, the results obtained from weight-loss tests in the absence and presence of 0.001 M in situ synthesized inhibitor, which had the best inhibition efficiency, are shown in Table 1. It can be seen that there is a considerable decrease in corrosion rate in the presence of inhibitors in comparison with the blank solution. Considering the optimum concentration of the 10^{-3} M inhibitor, the inhibition efficiency obtained from polarization studies is greater than weight-loss tests, 96% and 87%, respectively.

The adsorption behavior of the inhibitor molecules on the metal surface can be applied to explain the inhibition mechanism of inhibitors.[27] Several adsorption isotherms can be used to assess the adsorption behavior of the inhibitors. Langmuir isotherm is a suitable model, which is generally used for inhibitor studies. According to this model, the surface coverage (θ) is proportional to inhibitor concentration (C) as follows:[18,27]

$$\frac{\theta}{1-\theta} = K_{ads}C \quad (6)$$

By rearranging Equation (6):

$$\frac{C}{\theta} = \frac{1}{K_{ads}} + C \quad (7)$$

where K_{ads} is the equilibrium constant for adsorption reaction. This is a general model and has been used for inhibitor studies. The linear relationship of C/θ vs. C was displayed in Figure 5, which has a slope near 1, while the correlation coefficient, r, is close to 1, showing that the adsorption of in situ synthesized inhibitor on carbon steel surface can be well fitted to the Langmuir adsorption isotherm.

The intercept for the C/θ vs. C line was applied to calculate the adsorption equilibrium constant, and then the standard adsorption free energy (ΔG°_{ads}) was estimated from the following equation and listed in Table 2.

$$\Delta G^{\circ}_{ads} = -RT \ln(55.5\ K_{ads}) \quad (8)$$

where R is the gas constant and T is absolute temperature of the experiment. The large negative value for ΔG°_{ads} suggests that the inhibitor is adsorbed on the surface by a strong interaction between the inhibitor molecules and the mild steel surface.[28] It has been reported that the ΔG°_{ads} value up to –20 kJ/mol indicates a physical adsorption, while that more negative than –40 kJ/mol involves sharing or transfer of electron from the inhibitor molecules to the metal surface to form a coordinate-type bond (chemisorption).[17,29-30] As can be understood from Table 2, the value of ΔG°_{ads} is within –40 kJ/mol and –20 kJ/mol, indicating that the adsorption mechanism of the in situ synthesized inhibitor on carbon steel in H_2S-containing solution is typical of physisorption. The high value of K_{ads} reveals that the inhibitor possesses strong adsorption ability onto the carbon steel surface.[27]

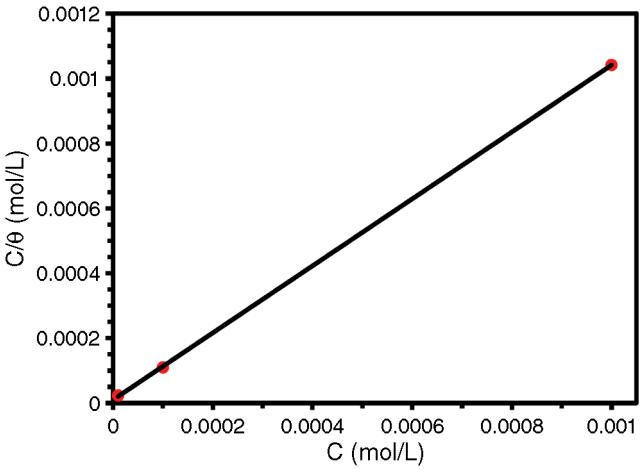

FIGURE 5. *Langmuir adsorption isotherm of the in situ synthesized inhibitor in H_2S-containing solution at 25°C.*

TABLE 2
Adsorption Parameters Calculated from the Langmuir Adsorption Isotherm

Solution	K_{ads} (M^{-1})	ΔG°_{ads} (kJ mol^{-1})	r
H_2S-containing solution with in situ synthesized inhibitor	10^{-3}	–38.5	0.99969

Electrochemical Impedance Spectroscopy

Electrochemical impedance spectroscopy (EIS) has been used to investigate the surface layer created by inhibitors. The effect of inhibitor concentration on the impedance behavior of mild steel in H_2S-containing solutions at 25°C has been exhibited in the form of Nyquist, Bode, and phase-angle plots and their fitted curves in Figures 6(a), (b), and (c), respectively.

Nyquist plots for carbon steel at various concentrations of in situ synthesized inhibitor are nearly similar and contain a depressed semicircle at higher frequencies that is related to the charge-transfer process. An increase in the semi-circle diameter is indicating an increase in corrosion resistance of carbon steel in the presence of inhibitors. It is observed that increasing the concentration of in situ synthesized

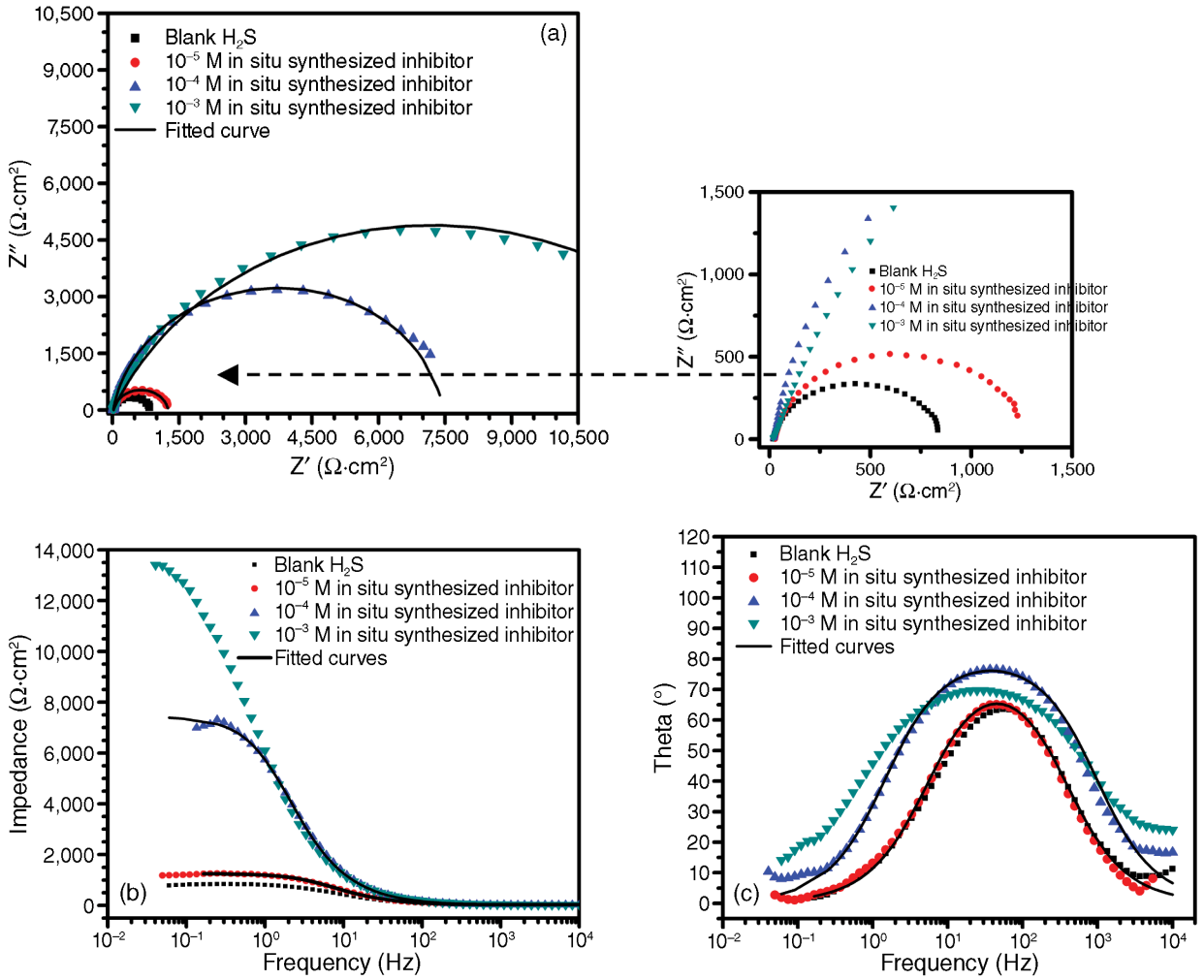

FIGURE 6. *Electrochemical impedance plots for carbon steel in H_2S-containing solution with different concentrations of in situ synthesized inhibitor at 25°C: (a) Nyquist, (b) Bode, and (c) phase-angle plots.*

inhibitor results in an increase in the size of the semicircle in Figure 6(a) and in the impedance of the interface in Figure 6(b), which indicate inhibition of the corrosion process.

The extracted impedance parameters, analyzed by EIS spectrum analyzer software from EIS plots, are listed in Table 3. Equivalent circuit that is used to fit the EIS data of mild steel is shown in Figure 7. Inhibitor efficiency can also be estimated by charge-transfer resistance according to the following formula:[17-18]

$$\%\eta = \frac{R - R^{o}}{R} \times 100 \qquad (9)$$

where R_0 and R are charge-transfer resistance of carbon steel in the absence and presence of the inhibitor, respectively. Calculated efficiency by charge-transfer resistance is in close correlation with those obtained from polarization results. Furthermore, values of CPE capacitance were calculated by the following equation:[31]

$$c_{dl} = P^{(\frac{1}{n})} R_{ct}^{(\frac{1-n}{n})} \qquad (10)$$

In the above expressions, P is the magnitude of CPE and n is the deviation parameter. Generally, the values of double-layer capacitance (C_{dl}) decrease by adding inhibitors. According to the Helmholtz model, C_{dl} is inversely proportional to the surface film thickness:[32]

$$c_{dl} = \frac{\varepsilon_o \varepsilon}{d} S \qquad (11)$$

where d is the thickness of the film, S is the surface of the electrode, ε_o is the permittivity of the air, and ε is the local dielectric constant. The values of C_{dl} decrease by increasing the concentration of in situ synthesized inhibitor. The decrease in the C_{dl} can be attributed to the decrease in local dielectric constant or an increase in the thickness of the electrical double layer, suggesting that in situ synthesized inhibitor

TABLE 3

Impedance Parameter Data and Linear Polarization Resistance Results for Carbon Steel in H_2S-Containing Solution Without and With Different Concentrations of In Situ Synthesized Inhibitor at 25°C

		EIS							LPR		
Inhibitor	Concentration	R_s ($\Omega \cdot cm^2$)	R_{ct} ($\Omega \cdot cm^2$)	P ($\mu F/cm^2$)	n	C_{dL}	θ	%η	R_p ($\Omega \cdot cm^2$)	θ	%η
Blank		18	828 (±8)	49	0.88	32	—	—	848 (±6)	—	—
In situ synthesized inhibitor	10^{-5} M	27	1,228 (±7)	33	0.90	23	0.32	32	1,265 (±4)	0.33	33
In situ synthesized inhibitor	10^{-4} M	20	7,438 (±19)	17	0.91	14	0.89	89	9,000 (±17)	0.90	90
In situ synthesized inhibitor	10^{-3} M	18	14,404 (±24)	30	0.78	10	0.94	94	14,505 (±23)	0.94	94

molecules function by adsorption at the interface of metal/solution.[17-18,27]

Corrosion Product Evaluation by Scanning Electron Microscopy and Energy-Dispersive Spectroscopy

Figure 8 depicts the morphologies of carbon steel specimens after immersion in H_2S-containing solution without and with 10^{-3} M in situ synthesized inhibitor. It can be clearly observed that in the absence of the inhibitor, the steel surface was seriously corroded with areas of uniform corrosion (Figure 8[a]). In the presence of the inhibitor, however, the specimen surface was more smooth (Figure 8[b]). This is because of the involvement of inhibitor molecules in the interaction with the reaction sites of the steel surface, resulting in a decrease in the contact between iron and the aggressive medium and sequentially exhibited excellent inhibition effect.[33-34]

According to Ma, et al.,[35] at the lower pH values (<2) iron dissolves via Reaction (12) and little iron sulfide forms because of the relatively greater solubility of the iron sulfide phases. In this case, H_2S only exhibits the acceleration effect on the dissolution of iron.

$$FeSH^+ + H_3O^+ \Rightarrow Fe^{2+} + H_2S + H_2O \qquad (12)$$

The composition of the layer on the surface was studied using EDS analysis and is represented in Figure 9, which detected the formation of FeS on the surface.

Fourier Transform Infrared Spectra

FTIR spectroscopy is a well-established characterization tool offering a "fingerprint" for chemical compounds.[36-37] The FTIR reflectance spectrum of the corrosion layer formed on the steel surface after immersion in H_2S-containing solution with 10^{-3} M in situ synthesized inhibitor and the 2-phenylbenzimidazole, which is synthesized in the laboratory, are shown in Figure 10(a).

The band at 3,446.1 cm^{-1} is attributed to N–H stretching and 1,646 cm^{-1} is for C=N stretching. The

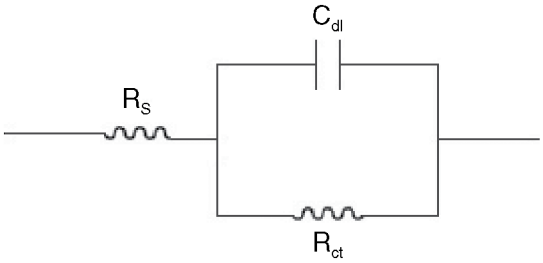

FIGURE 7. *Electrochemical equivalent circuit used for simulation of impedance spectra.*

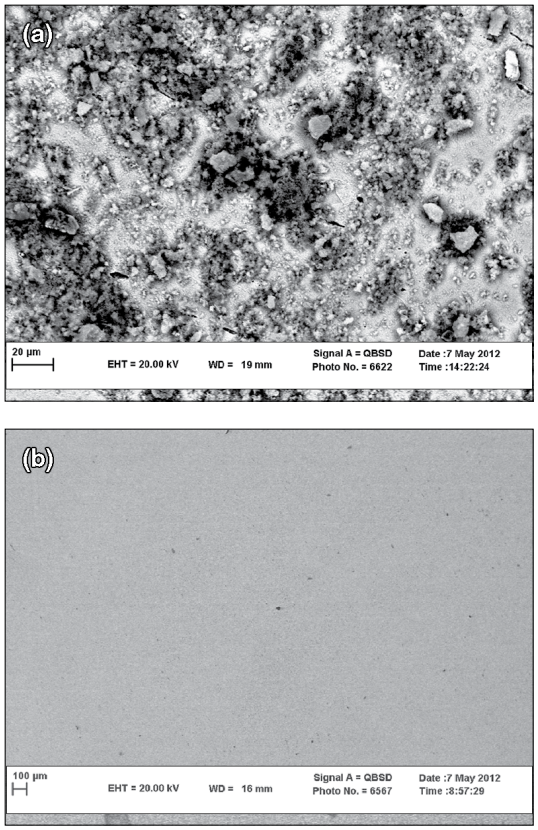

FIGURE 8. *SEM images for carbon steel surface: (a) H_2S-containing solution and (b) H_2S-containing solution with 10^{-3} M in situ synthesized inhibitor.*

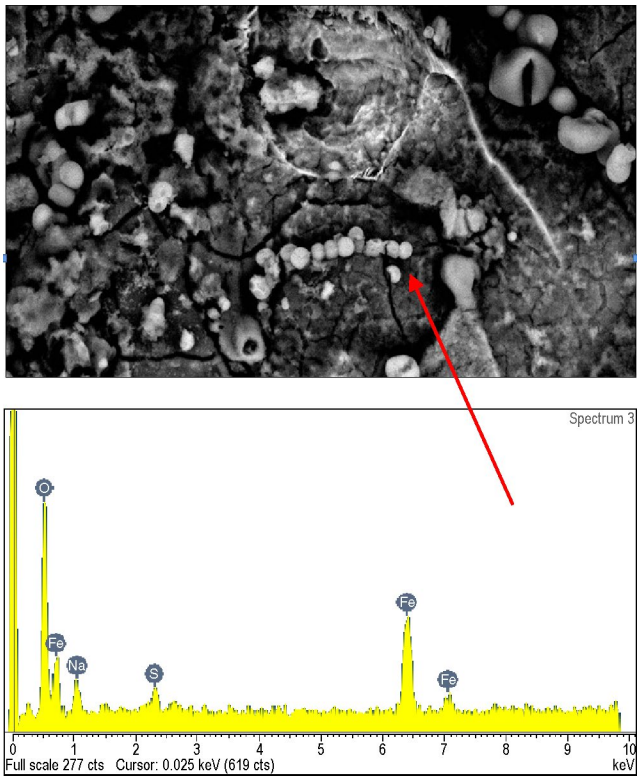

FIGURE 9. *EDS analysis of the corrosion layer.*

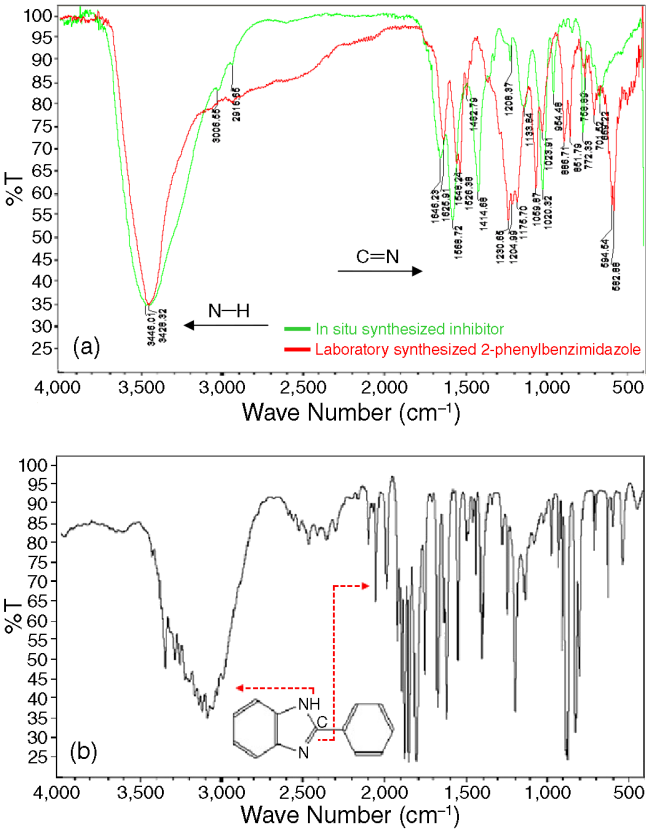

FIGURE 10. *(a) FTIR spectra of carbon steel after immersion in H_2S-containing solution with 10^{-3} M in situ synthesized inhibitor; (b) FTIR spectra for the commercial 2-phenylbenzimidazole.*

other peaks are for C–H aromatic bands.[37] As it is shown in the molecular structure and FTIR spectra for the commercial 2-phenylbenzimidazole in Figure 10(b), these kinds of bands are typical for this material. So, we can conclude that this organic compound is produced with the in situ manner on the metal surface in a H_2S-containing solution.

Quantum Chemical Calculations

Being clear that the layer which was deposited on the metal surface was 2-phenylbenzimidazole with FTIR techniques, we investigated the correlation between molecular structure of this organic compound and its inhibition effect with quantum chemical study. So, geometric structures and electronic properties of 2-phenylbenzimidazole has been calculated by a DFT method using the B3LYP level and 3-21G** basis set. These analyses have been used for benzaldehyde and benzene-1,2-diamine, too.

Figures 11 and 12 show optimized molecular structures, HOMO and LUMO of 2-phenylbenzimidazole, and reveal that the benzene ring and N atoms have larger electronic density. The type of benzene ring electrons is π-bonding electrons, while for N atoms those are non-bonding electrons pair. It is suggested that the benzene ring and N atoms can be suitable places for adsorption onto the surface, especially in the case of N atoms because they have lone pairs of electrons.[18] Molecules of the present inhibitor can be adsorbed directly at the steel surface on the basis of donor acceptor interactions between π-electrons of the benzene ring, nonbonding lone pairs of N atoms, and vacant d-orbitals of iron atoms.

Quantum chemical indexes containing E_{HOMO}, E_{LUMO}, ΔE ($\Delta E = E_{LUMO} - E_{HOMO}$), and dipole moment (μ) for the studied molecules are presented in Table 4. It has been reported that excellent inhibition corrosion properties are usually obtained using organic compounds that not only offer electrons to unoccupied orbitals of the metal but also accept free electrons from the metal by using their anti-bond orbitals to form stable chelates.[17-18] By looking at Figure 11, it is understandable that this inhibitor also could accept the d-orbital electrons of iron by LUMO on the benzene ring and N atoms. Consequently, this electron acceptance could help to form a more stable bond between the inhibitor molecule and the iron surface.

We can mention the energy of HOMO that is often associated with the electronic donating ability of a molecule. Therefore, an increase in the values of E_{HOMO} can facilitate the adsorption and therefore the inhibition efficiency, by indicating the disposition of the molecule to donate orbital electrons to an appropriate acceptor with empty molecular orbitals.[38-39] The energy of LUMO on the other hand, indicates the

ability of the molecule to accept electrons. The lower the value of E_{LUMO}, the more probable it is that the molecule accepts electrons.[38] In the same way, low values of the energy of the gap, $\Delta E = E_{LUMO} - E_{HOMO}$, will render good inhibition efficiencies, because the energy to remove an electron from the last occupied orbital will be low.[40] Increasing values of the dipole moment has been reported to facilitate adsorption (and therefore inhibition) by influencing the transport process through the adsorbed layer. So, the inhibition efficiency increases with increasing values of the dipole moments.[38]

Table 4 data reveal that although 2-phenylbenzimidazole does not get the highest E_{HOMO} and the lowest E_{LUMO}, it has the smaller energy gap ($\Delta E = E_{LUMO} - E_{HOMO}$) and the greater dipole moment (μ) as compared to other molecules, which indicate the better inhibition efficiency than its components.

CONCLUSIONS

❖ Data obtained from weight-loss, polarization, and EIS measurements represented that in situ synthesis of the inhibitor has a great effect on achieving high corrosion inhibition efficiencies for carbon steel in H_2S-containing solutions. The beneficial condition among the in situ synthesized inhibitor's concentration was 10^{-3} M with the approximate efficiency of 96%. Adsorption of this inhibitor obeys Langmuir rule and calculated standard adsorption free energy shows physical adsorption for this inhibitor. SEM results demonstrated the severe deterioration of the surface in the absence of inhibitor. The results obtained from FTIR spectra proved that 2-phenybenzimidazole synthesized on the metal surface from the combination of benzene-1,2-diamine and benzaldehyde along with ferric chloride catalyst in electrolyte solution. Quantum chemical study reveals that the benzene ring and N atoms can be suitable sites for adsorption onto the surface. This is pronounced for N atoms because of having a lone pair of electrons. Additionally, 2-phenybenzimidazole has the smaller energy gap ($\Delta E = E_{LUMO} - E_{HOMO}$) and the greater dipole moment (μ) as compared to its components, which indicate the better inhibition efficiency.

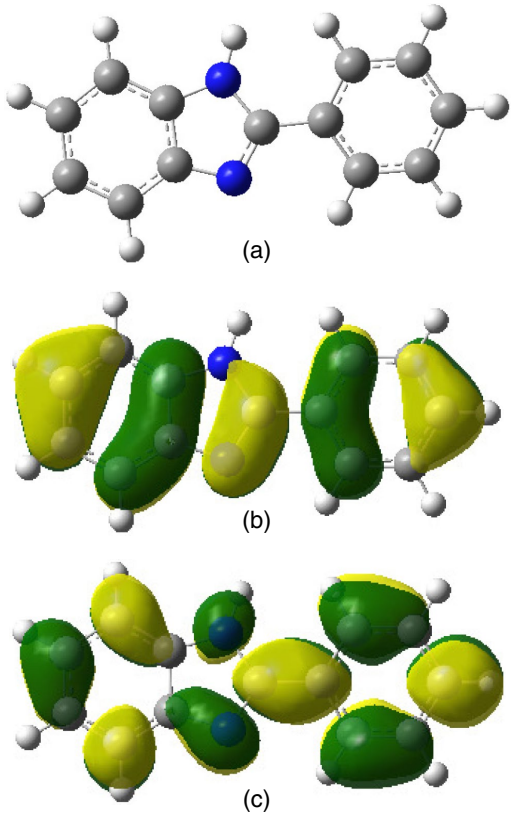

FIGURE 11. *(a) Molecular structure, (b) HOMO, and (c) LUMO of 2-phenylbenzimidazole.*

REFERENCES

1. J.G. Gonzalez-Rodriguez, T. Zeferino-Rodriguez, D.M. Ortega, S. Serna, B. Campillo, M. Casales, E. Valenzuela, J.A. Juárez-Islas, *Int. J. Electrochem. Sci.* 2 (2007): p. 883-896.
2. M.B. Kermani, A. Morshed, *Corrosion* 59 (2003): p. 659.
3. E.F. Diaz, J.G. Gonzalez-Rodriguez, R. Sandoval-Jabalera, S. Serna, B. Campillo, M.A. Neri-Flores, C. Gaona Tiburcio, A. Martinez-Villafañe, *Int. J. Electrochem. Sci.* 5 (2010): p. 1821-1836.
4. Y.S. Choi, S. Nešić, Sh. Ling, *Electrochim. Acta* 56 (2011): p. 1752-1760.
5. M. Bonis, M. Girgis, K. Goerz, R. MacDonald, "Weight Loss Corrosion with H_2S: Using Past Operations for Designing Future Facilities," CORROSION 2006, paper no. 06122 (Houston, TX: NACE International, 2006).
6. R.K. Vagapov, V.S. Bizyaeva, V.I. Kichigin, *Prot. Met.* 43 (2007): p. 643-647.
7. J. Tang, Y. Shao, J. Guo, T. Zhang, G. Meng, F. Wang, *Corros. Sci.* 52 (2010): p. 2050-2058.
8. S.N. Smith, M. Joosten, "Corrosion of Carbon Steel by H_2S in CO_2 Containing Oilfield Environments," CORROSION 2006, paper no. 06115 (Houston, TX: NACE, 2006).
9. D.B. Kudryavtsev, A.R. Panteleeva, A.V. Yurina, S.S. Lukashenko, Yu.P. Khodyrev, R.M. Galiakberov, D.N. Khaziakhmetov, L.A. Kudryavtseva, *Petrol. Chem.* 49 (2009): p. 193-198.
10. S. Aezola, J. Genesca, *J. Solid State Electrochem.* 8 (2005): p. 197-200.
11. H.Y. Ma, X.L. Cheng, S.H. Chen, G.Q. Li, X. Chen, S.B. Lei, H.Q. Yang, *Corrosion* 54 (1998): p. 634-640.
12. H. Ma, X. Cheng, S. Chen, C. Wang, J. Zhang, H. Yang, *J. Electroanal. Chem.* 451 (1998): p. 11-17.
13. H. Ma, X. Cheng, G. Li, S. Chen, Z. Quan, S. Zhao, L. Niu, *Corros. Sci.* 42 (2000): p. 1669-1683.
14. X.L. Cheng, H.Y. Ma, J.P. Zhang, X. Chen, S.H. Chen, H.Q. Yang, *Corrosion* 54 (1998): p. 369-376.
15. B.M. Miksic, A.Y. Furman, M.A. Kharshan, "Effectiveness of the Corrosion Inhibitors for the Petroleum Industry Under Various Flow Conditions," CORROSION 2009, paper no. 09573 (Houston, TX: NACE, 2009).
16. S. Lin, L. Yang, *Tetrahedron Lett.* 46 (2005): p. 4315-4319.
17. N.S. Ayati, S. Khandandel, M. Momeni, M.H. Moayed, A. Davoodi, M. Rahimizadeh, *Mater. Chem. Phys.* 126 (2011): p. 873-879.
18. A. Kosari, M. Momeni, R. Parvizi, M. Zakeri, M.H. Moayed, A. Davoodi, H. Eshghi, *Corros. Sci.* 53 (2011): p. 3058-3067.
19. Sh. Pournazari, M.H. Moayed, M. Rahimizadeh, *Corros. Sci.* 71 (2013): p. 20-31.
20. H. Eshghi, M. Rahimizadeh, A. Shiri, P. Sedaghat, *Korean Chem. Soc.* 33 (2012): p. 515-518.
21. G.F. Chen, X.Y. Dong, *E-Journal of Chem.* 9 (2012): p. 289-293.
22. J. Aljourani, K. Raeissi, M.A. Golozar, *Corros. Sci.* 51 (2009): p. 1836-1843.
23. M. El Azhar, B. Mernari, M. Traisnel, F. Bentiss, M. Lagrenée, *Corros. Sci.* 43 (2001): p. 2229-2238.

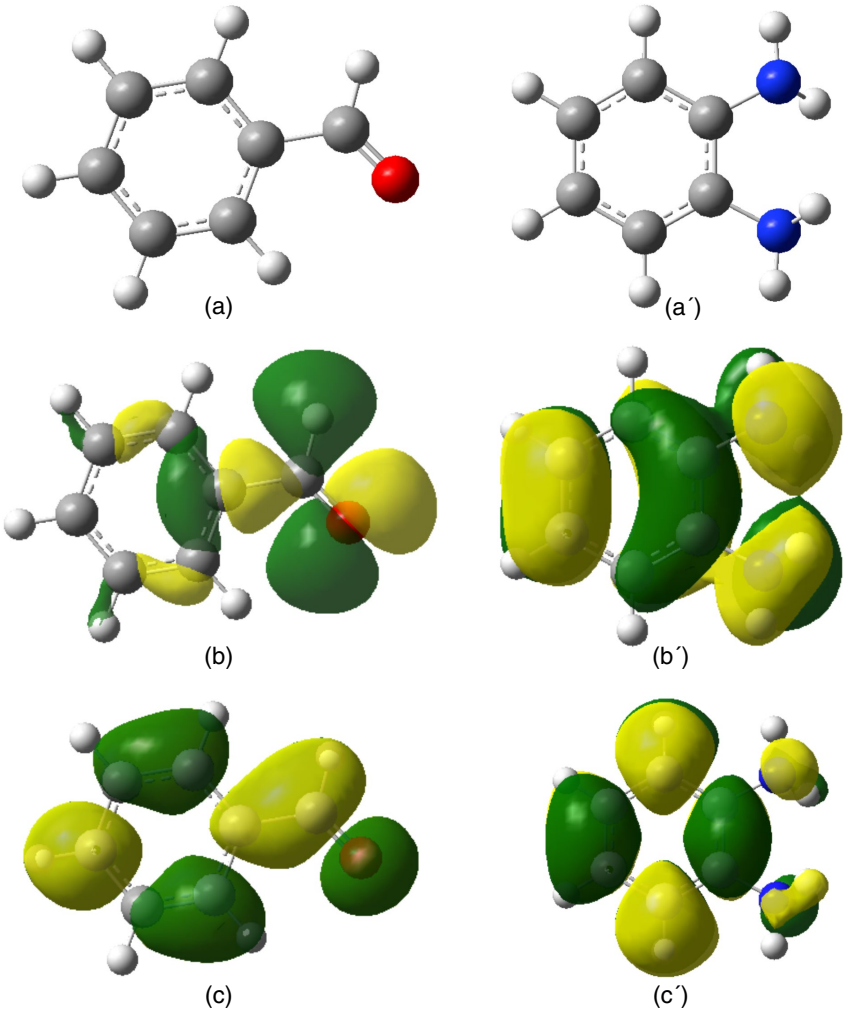

FIGURE 12. *(a) Molecular structure, (b) HOMO, and (c) LUMO of benzaldehyde; (a′) molecular structure (b′) HOMO, and (c′) LUMO of benzene-1,2-diamine.*

TABLE 4
HOMO and LUMO Values of the Examined Molecules Calculated by DFT Method

Quantum Chemical Parameters	2-Phenylbenzimidazole	Benzene-1,2-Diamine	Benzaldehyde
E_{HOMO}	–5.95	–5.24	–7.15
E_{LUMO}	–1.44	0.91	–1.93
$\Delta E = E_{LUMO} - E_{HOMO}$	4.51	5.44	5.22
Dipole moment	3.13	1.38	2.99

24. X. Wang, H. Yang, F. Wang, *Corros. Sci.* 53 (2011): p. 113-121.
25. J. Liu, Y. Lin, X. Yong, X. Li, *Corrosion* 61 (2005): p. 1061-1069.
26. M.L. Doche, J.Y. Hihn, A. Mandroyan, R. Viennet, F. Touyeras, *Ultrason. Sonochem.* 10 (2003): p. 357-362.
27. X. Wang, H. Yang, F. Wang, *Corros. Sci.* 53 (2011): p. 113-121.
28. M.S. Morad, *Corros. Sci.* 50 (2008): p. 436-448.
29. O. Benali, L. Larabi, M. Traisnel, L. Gengembra, Y. Harek, *Appl. Surf. Sci.* 253 (2007): p. 6130-6139.
30. F. Bentiss, M. Lebrini, M. Lagrenée, *Corros. Sci.* 47 (2005): p. 2915-2931.
31. B. Hirschorn, M.E. Orazem, B. Tribollet, V. Vivier, I. Frateur, M. Musiani, *Electrochim. Acta* 55 (2010): p. 6218-227.
32. H.H. Hassan, *Electrochim. Acta* 51 (2006): p. 5966-2972.
33. S. Muralidharan, K.L.N. Phani, S. Pitchumani, S. Ravichandran, S.V.K. Iyer, *J. Electrochem. Soc.* 142 (1995): p. 1478-1483.
34. R.A. Prabhu, T.V. Venkatesha, A.V. Shanbhag, G.M. Kulkarni, R.G. Kalkhambkar, *Corros. Sci.* 50 (2008): p. 3356-3362.
35. H. Ma, X. Cheng, G. Li, Sh. Chen, Zh. Quan, Sh. Zhao, L. Niu, *Corros. Sci.* 42 (2000): p. 1669-1683.
36. X. Li, Sh. Deng, H. Fu, G. Mu, N. Zhao, *Appl. Surf. Sci.* 254 (2008): p. 5574-5586.
37. D. Pavia, G. Lampman, G. Kriz, *Introduction to Spectroscopy* (Stamford, CT: Thomson Learning, 2001).
38. I.B. Obot, N.O. Obi-Egbedi, *Corros. Sci.* 52 (2010): p. 657-660.
39. Gokhan Gece, *Corros. Sci.* 50 (2008): p. 2981-2992.
40. K.F. Khaled, *Electrochim. Acta* 48 (2003): p. 2493-2503.